Optimal Current Control of a Wireless Power Transfer System for High Power Efficiency

Jaegue Shin[1], Seungyong Shin, Yangsu Kim, Seokhwan Lee, Boyune Song and Guho Jung

Center for wireless power transfer technology, KAIST
291 Daehak-ro, Yuseong-gu, Daejeon, Korea
[1]jkshin@kaist.ac.kr

***Abstract*— This paper introduces the composition and the power loss model of a wireless power transfer system. By the measured power loss parameters and experimental results, the optimal current control for the maximum power transfer efficiency is proposed.**

***Keywords*— wireless power transfer, power loss, power transfer efficiency, experiment, model analysis**

I. INTRODUCTION

Electric equipment is usually powered through an electrical wire that transfers electric power. However, the wire is very uncomfortable because the equipment cannot move during powering or charging. Although battery is used for the mobility of electric equipment, some limits of the battery such as size, weight, capacity, inconvenience of charging and so on are not solved enough.

To overcome the problems, wireless power transfer technology has been developed over the past few decades. Using inductive coupling, a wireless power transfer system transmits power without mechanical contacts. The wireless power transfer technology is used in wide-ranging applications from cell phone [1-2] to electric vehicle [3-5].

One of the most important applications is electric vehicle. For the environmental pollution and fossil fuel depletion, electric vehicle is considered as an effective solution. However, the battery for electric vehicle has very large size and weight to charge enough energy for the vehicle. This problem increase the battery cost and lower the energy efficiency.

To solve the problem, Online Electric Vehicle (OLEV) system that charges moving vehicles on a roadway has been developed by Korea Advanced Institute of Science and Technology (KAIST) [6-10]. Fig. 1 shows the concept of the OLEV system. The OLEV system uses the power line rail underneath the roadway to charge the moving vehicles. Since the charging on roadway reduces the required capacity of battery, size, weight and price of the battery can be scaled down. Furthermore, problems of the conservative electric vehicles, for example, long charging time and short driving rage can be improved.

To be commercialized, the power transfer efficiency issue must be considered for economic reasons. The power transfer efficiency of the wireless power transfer system varies depending on the control of the current. Hence, optimal current control for maximum power transfer efficiency must be considered by analysing power loss model. In this paper, the wireless power transfer system is introduced and the power loss model is analysed. Through model analysis and experiment, the optimal current for maximum power transfer efficiency is proposed.

II. WIRELESS POWER TRANSFER SYSTEM

Wireless power transfer systems using inductive coupling can be classified into two types. One type uses magnetic core and the other does not. The magnetic core has the advantage of increasing the power transfer capacity and the disadvantage of the cost, weight and core loss. Therefore, high power wireless transfer systems use magnetic cores and low power systems use non-core method generally.

A wireless power transfer system is comprised of a power transmitter part and a power receiver part. The power transmitter part includes an inverter and primary coils. The inverter sends a current to the primary coils. Then, the primary coils generate magnetic flux that transfers power to the power receiver part. The power receiver part includes a pick-up module and a regulator. The pick-up module receives the magnetic flux and generates power. The regulator stabilizes the output power by controlling the voltage and current of the pick-up module.

The inverter usually designed to provide constant current to consider variations in the load resistance. A misalignment between the power transmitter part and the power receiver part or multi pick-ups charging cause the variations in the load, and this brings out a power decrease. Thus, the inverter provides steady magnetic flux by the constant current control.

Contrary to the inverter control, the regulator may change the current of the pick-up to adjust the output power. Higher pick-up current allows higher output power. However, high current also gives rise to power loss such as core loss, winding copper loss, parasitic resistance loss and so on.

III. POWER LOSS MODEL

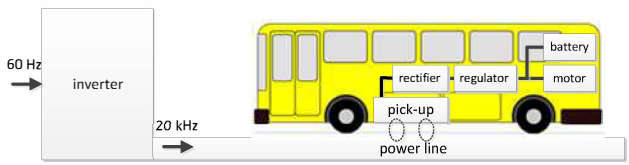

Fig. 1. Concept of the Online Electric Vehicle system.

978-1-4673-1372-8/12/$31.00 ©2012 IEEE

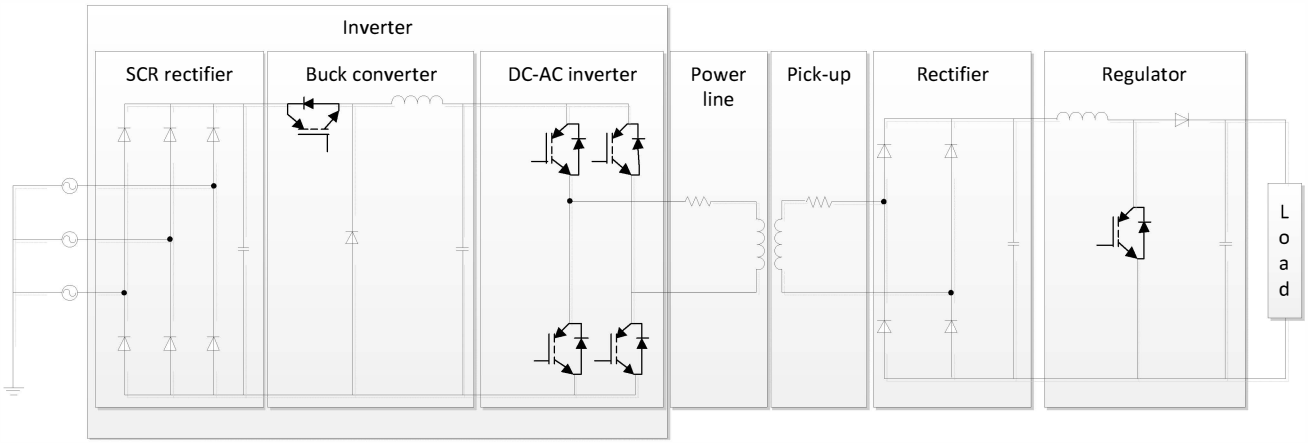

Fig. 2. Simplified circuit of the overall OLEV system.

In this section, the power model is presented along with an example of the OLEV system. Fig. 2 shows a simplified circuit of the overall OLEV system. The inverter converts 60 Hz (in Korea) power to the constant current at 20 kHz operation frequency of the system. The inverter consists of a SCR rectifier, a DC-DC buck converter and an IGBT DC-AC inverter. The power losses of the components are calculated by

$$P_{rec\_1} = R_{rec\_1} I_0^2 + V_{rec\_1} I_0 \quad (1)$$

$$P_{DC} = C_{DC} \cdot V_{DC}^2 \cdot f_{buck} + R_{DC} I_1^2 + V_{DC} I_1 \quad (2)$$

$$P_{AC} = C_{AC} \cdot V_{AC}^2 \cdot f \quad (3)$$

where P_{rec_1}, P_{DC} and P_{AC} are the power losses of the rectifier, the DC-DC converter and the DC-AC inverter. I_0 and I_1 are the input and output currents of the DC-DC converter. R_{rec_1}, R_{DC}, V_{rec_1} and V_{DC} are the parasitic resistances and a voltage drops of the rectifier and the DC-DC converter, respectively. C_{DC} and C_{AC} are the effective switching capacitances of the IGBTs of the DC-DC converter and DC-AC inverter. V_{DC} and V_{AC} are the voltages across the IGBTs. f_{buck} is the switching frequency of the buck converter and f is the operation frequency 20 kHz. The power loss of the primary coil, P_{coil_1}, is calculated by

$$P_{coil\_1} = R_{coil\_1} I_1^2 \quad (4)$$

where R_{coil_1} is the resistance of the primary coil. These power losses are complex and difficult to be obtained by device parameters. However, the losses in (1), (2), (3) and (4) are fixed because the currents and frequencies are controlled to be constant, and they can be obtained easily by experiments. These power losses can be summated into a fixed power loss, P_{const}.

The pick-up loss is compromised of the magnetic core loss and winding loss. The core loos P_{core} and the winding loss $P_{winding}$ are calculated by

$$P_{core} = k \cdot f^{\alpha} \cdot B^{\beta} \cdot M \quad (5)$$

$$P_{winding} = R_{coil\_2} I_2^2 \quad (6)$$

where k, α and β are curve fitting coefficients. f is the operating frequency 20 kHz, B is the maximum peak magnetic flux density and M is the volume of magnetic core. R_{coil_2} is the resistance of secondary coil in the pick-up and I_2 is the pick-up current.

The core loss is proportional to f^{α} and B^{β}. Since B is roughly proportional to the pick-up current I_2 and the empirically obtained value of β is near 2, the core loss is approximately proportional to I_2^2.

The rectifier converts AC power to DC using diodes, and the regulator is a boost converter that controls the voltage and the current of the pick-up. Power losses of the rectifier and the regulator are calculated by

$$P_{rec\_2} = R_{rec\_2} I_2^2 + V_{rec\_2} I_2 \quad (7)$$

$$P_{reg} = C_{reg} \cdot V_{reg}^2 \cdot f_{boost} + R_{reg} I_3^2 + V_{reg} I_3 \quad (8)$$

where I_2 and I_3 are the input and output currents of the boost converters. R_{rec_2}, R_{reg}, V_{rec_2} and V_{reg} are the parasitic resistances and a voltage drops of the rectifier and the regulator in the power receiver part, respectively. C_{reg} and V_{reg} are the effective switching capacitances of the IGBTs of the boost converter and the voltages across the IGBTs. f_{boost} is the switching frequency of the boost converter.

The duty ratio of the boost converter is controlled to adjust the output power, and then I_2 and I_3 are determined. Therefore, I_3 is not independent of I_2 but a function of I_2. If I_2 is controlled by the regulator to a fixed value, I_3 is fixed too. Accordingly, the power losses of the pick-up, the rectifier and

TABLE I
THE POWER LOSS PARAMETERS OF THE OLEV SYSTEM

Parameters	Value
P_{const}	7.07
k_1	0.24
k_2	0.016

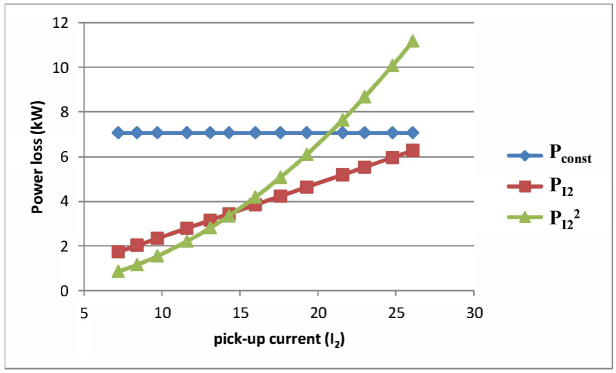

Fig. 3. P_{const}, P_{I2} and P_{I2}^2 as functions of I_2

the regulator in (5), (6), (7) and (8) vary depending on I_2 only because other parameters are fixed.

For the entire power losses, the all terms in (1), (2), (3), (4), (5), (6), (7) and (8) can be classified into three types: the constant power loss P_{fix}, the loss proportional to I_2 and the loss proportional to I_2^2. Therefore, the total power loss P_{loss} is expressed by

$$\begin{aligned} P_{loss} &= P_{const} + P_{I_2} + P_{I_2^2} \\ &= P_{const} + k_1 I_2 + k_2 I_2^2 \end{aligned} \tag{9}$$

where P_{const}, P_{I2} and P_{I2}^2 are the constant power loss, I_2 proportional power loss and I_2^2 proportional power loss. k_1 and k_2 are power loss coefficient.

The parameters of the OLEV system are obtained by experiments and shown in Table I, and Fig. 3 shows P_{const}, P_{I2} and P_{I2}^2 as functions of pick-up current I_2 according to the parameters. Although P_{const} is dominant at low current, a sum of P_{I2} and P_{I2}^2 is much larger at high current.

IV. EXPERIMENTAL RESULTS

For experiments, we implemented the OLEV system in a laboratory environment. In the system, the inverter was designed to convert a three-phase 60 Hz power to a single-phase 20 kHz constant current of 260 A. The implementation of the inverter is presented in Fig. 5(a). The ferrite core blocks were installed in the power line module to maximize the magnetic flux as shown in Fig. 5(b). The pick-up module was comprised of ferrite cores and winding cables as shown in Fig. 4(a). A boost converter in Fig. 4(b) was designed and used as a regulator that controls the voltage and the current of the pick-up.

(a) (b)

Fig. 5. The implementation of (a) the inverter and (b) the power line.

(b) (b)

Fig. 4. The implementation of (a) pick-up module and (b) regulator

We measured the output power and the power transfer efficiency of the whole system by a power analyser. The total power transfer efficiency of the system η is calculated by

$$\eta = \frac{P_{output}}{P_{output} + P_{loss}} \tag{10}$$

where P_{output} is the output power capacity of the whole system. Fig. 6 shows P_{output}, P_{loss} and η measured at various pick-up currents. As the pick-up current increase, the output power and the power loss increase too. While the output power increases almost linearly to the pick-up current, the power loss

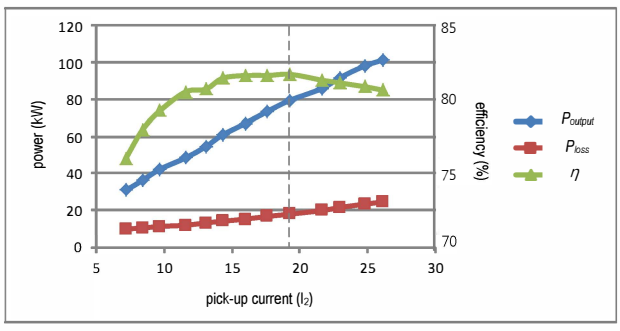

Fig. 6. P_{output}, P_{loss} and η versus I_2.

increases exponentially because of P_{12}^2 term. The maximum efficiency was 81.7% at 79.5 kW output power with a 19.3 A pick-up current. At the maximum power 101.2 kW, the efficiency was 80.6% and the pick-up current was 26.1 A. Therefore, in this system, we have two options: a high power charging and a high efficiency charging. If high power is needed for fast charging or high-speed driving, it is better to control the pick-up current at the maximum. However, if low power is enough, the optimal pick-up current is recommended to maximize the power transfer efficiency.

V. Conclusions

This paper presented the power loss model of a wireless power transfer system and the power loss parameters measured by experiments. The power losses on the pick-up current controls were analyzed. Through the experiments, the output power and power loss were measured and the power transfer efficiency was calculated. The optimal pick-up current control that achieves the maximum efficiency was proposed when the maximum power is not needed.

References

[1] C. Kim, D. Seo, J. You, J. Park and B. H. Cho, "Design of a contactless battery charger for cellular phone," *IEEE Trans. Ind. Electron.,* vol. 48, no. 6, pp. 1238-1247, Dec. 2001.

[2] B. Choi, J. Nho, H. Cha, T. Ahn and S. Choi, "Design and Implementation of Low-Profile Contactless Battery Charger Using Planar Printed Circuit Board Windings as Energy Transfer Device," *IEEE Trans. Ind. Electron.,* vol. 51, no. 1, pp. 140-147, Feb. 2004.

[3] J. L. Villa, J. Sallan, A. Llombart and J.F. Sanz, "Design of a high frequency inductively coupled power transfer system for electric vehicle battery charge," *Appl. Energy*, vol. 86, no. 3, pp. 355–363, Mar. 2009.

[4] C. Wang, O.H. Stielau and G. A. Covic, "Design considerations for a Contactless Electric Vehicle Battery Charger," *IEEE Trans. Ind. Electron.*, vol. 52, no. 5, pp. 1308–1314, Oct. 2005.

[5] J. Sallan, J. L. Villa, A. Llombart and J.F. Sanz, "Optimal design of ICPT systems applied to electric vehicle battery charge," *IEEE Trans. Ind. Electron.*, vol. 56, no. 6, pp. 2140–2149, Jun. 2009.

[6] J. Shin, B. Song, S. Lee, S. Shin, Y. Kim, G. Jung and S. Jeon, "Contactless power transfer systems for on-line electric vehicle (OLEV)," in *Proc. IEEE Int. Electric Vehicle Conf.*, pp. 1-4, Mar. 2012.

[7] B. Song, J. Shin, S. Lee, S. Shin, Y. Kim, S. Jeon and G. Jung, "Design of a high power transfer pickup for on-line electric vehicle (OLEV)," in *Proc. IEEE Int. Electric Vehicle Conf.*, pp. 1-4, Mar. 2012.

[8] S. Shin, J. Shin, Y. Kim, S. Lee, B. Song, G. Jung and S. Jeon, "Hybrid inverter segmentation control for online electric vehicle," in *Proc. IEEE Int. Electric Vehicle Conf.*, pp. 1-6, Mar. 2012

[9] Y. Kim, Y. Son, S. Shin, J. Shin, B. Song, S. Lee, G. Jung and S. Jeon, "Design of a regulator for multi-pick-up systems through using current offsets," in *Proc. IEEE Int. Electric Vehicle Conf.*, pp. 1-6, Mar. 2012.

[10] G. Jung, B. Song, S. Shin, S. Lee, J. Shin, Y. Kim, S. Jeon and D. Cho, "High efficient inductive power supply and pickup system for on-line electric bus," in *Proc. IEEE Int. Electric Vehicle Conf.*, pp. 1-5, Mar. 2012.